

Article

A Wearable Internet of Things Device for Noninvasive Remote Monitoring of Vital Signs Related to Heart Failure

Sheikh Muhammad Asher Iqbal ^{1,2}, Mary Ann Leavitt ³ , Imadeldin Mahgoub ¹  and Waseem Asghar ^{1,2,4,*} 

- ¹ Department of Electrical Engineering & Computer Science, Florida Atlantic University, Boca Raton, FL 33431, USA; siqbal2019@fau.edu (S.M.A.I.); mahgoubi@fau.edu (I.M.)
- ² Asghar-Lab, Micro and Nanotechnology in Medicine, College of Engineering and Computer Science, Boca Raton, FL 33431, USA
- ³ Christine E. Lynn College of Nursing, Florida Atlantic University, Boca Raton, FL 33431, USA; mleavit3@health.fau.edu
- ⁴ Department of Biological Sciences (Courtesy Appointment), Florida Atlantic University, Boca Raton, FL 33431, USA
- * Correspondence: wasghar@fau.edu

Abstract: Cardiovascular disease is one of the leading causes of death in the world. Heart failure is a cardiovascular disease in which the heart is unable to pump sufficient blood to fulfill the body's requirements and can lead to fluid overload. Traditional solutions are not adequate to address the progression of heart failure. Herein, we report a body-mounted wearable sensor to monitor the parameters related to heart failure. These include heart rate, blood oxygen saturation, thoracic impedance, and activity status. The device is compact and wearable and measures the parameters continuously in real time. The device is an Internet of Things (IoT) device connected with a cloud-based database enabling the parameters to be visualized on a mobile application.

Keywords: cardiovascular disease; heart failure; wearable sensor; thoracic impedance; heart rate; activity status; Internet of Things; telemedicine



Citation: Iqbal, S.M.A.; Leavitt, M.A.; Mahgoub, I.; Asghar, W. A Wearable Internet of Things Device for Noninvasive Remote Monitoring of Vital Signs Related to Heart Failure. *IoT* **2024**, *5*, 155–167. <https://doi.org/10.3390/iot5010008>

Academic Editor: Amiya Nayak

Received: 15 January 2024

Revised: 22 February 2024

Accepted: 28 February 2024

Published: 12 March 2024



Copyright: © 2024 by the authors. Licensee MDPI, Basel, Switzerland. This article is an open access article distributed under the terms and conditions of the Creative Commons Attribution (CC BY) license (<https://creativecommons.org/licenses/by/4.0/>).

1. Introduction

Cardiovascular diseases are related to heart and blood diseases [1]. They account for one-third of the deaths around the world with more than half a billion people affected. Heart failure (HF) is a serious cardiovascular disease with approximately 56.19 million cases around the world and 6.5 million in the US alone [2,3]. In this condition, the heart cannot pump a sufficient amount of blood to meet the requirements of the body. This lack of blood supply can lead to fluid overload and pulmonary edema, whereby fluid builds up in the lungs [4]. There are two main types: HF with preserved ejection fraction (HFpEF), also known as diastolic HF, and HF with reduced ejection fraction (HFrEF), also known as systolic HF [5]. In HFpEF, the heart pumps 50% or more of the amount of blood in the left ventricle, whereas in reduced ejection fraction less than or equal to 40% of blood is ejected. HF is difficult to treat completely however it can be managed by guideline-directed medical therapy and monitoring significant parameters [5]. These include heart rate (HR), oxygen blood saturation (SPO₂), thoracic impedance, and activity status of the subject. Current solutions for managing HF are implantable cardioverter defibrillators (ICDs) and CardioMEMS [6]. An ICD is an invasive solution in which a device is implanted inside the chest and used to monitor parameters related to HF, as well as treating irregular heart rhythms. The HF management program from Medtronic utilizes one such ICD that monitors parameters including HR, heart rate variability (HRV), activity status, and thoracic impedance [7–9]. CardioMEMS is another invasive device that monitors the progression of HF using pulmonary artery pressure [8,10].

These devices not only have surgical risks but are also very expensive. According to one estimate, an ICD costs approximately USD 37,000 and CardioMEMS costs approximately USD 17,750 [11,12] and, therefore, are not accessible for all HF patients. Moreover, ICDs are only recommended for patients with HFrEF. Therefore, there is a need for a cost-effective solution that is accessible to all HF patients. According to the World Health Organization (WHO), diagnostic tools should be in accordance with the ASSURED criteria, whereby ASSURED stands for affordable, sensitive, specific, user-friendly, rapid and robust, equipment-free, and deliverable devices. Internet of Things (IoT)-based wearable devices are one such solution that can provide continuous real-time monitoring and in accordance with the ASSURED criteria [13–15]. IoT is an integration of different things, such as sensors and software, embedded together for exchanging useful data over the Internet [16]. IoT allows for remote monitoring that not only provides timely monitoring and diagnosis but also has the potential to reduce healthcare costs [17]. Wearable devices have been found to be an effective tool for the use of IoT in healthcare [18]. Recently, efforts have been made for using wearable devices for various medical applications. Some efforts have also been made for the use of wearable devices specifically for HF management and monitoring [19–22]. Notable examples include a wearable vest for HF monitoring, a hemotag, and a wearable belt for monitoring vital cardiovascular parameters [23–25]. The wearable belt by Svagard et al. is a chest-based belt that measures transthoracic impedance (TTI) and weight to monitor HF [23]. They have found TTI to be 76% sensitive enough to HF and 33% sensitive to body weight. However, this device is not only bulky for the patient, but it is not a real-time continuous monitor, as it is only required to be used for 10 minutes to extract parameters. Moreover, it is not fully wearable in nature such that it cannot be used at all times and in all conditions, as it is only required to be used in resting conditions. Similarly, a hemotag can only be used in a resting position [24]; it monitors HF using time-synchronized vibrations from the chest for only 30 secs. Moreover, the wearable belt by Svagard et al. is a multiparametric belt for monitoring different vital cardiovascular parameters, such as heart rate and activity level, along with other vital parameters, including skin temperature, but does not include the most specific HF parameter, thoracic impedance [25]. Thoracic impedance is a vital indicator for measuring fluid accumulation and is a specific diagnostic indicator for HF. Herein, we report a wearable device that can monitor vitals related to HF in different real-time conditions at all times.

The device measures parameters such as thoracic impedance, oxygen saturation in blood (SPO₂), HR, and activity status. Thoracic impedance is the electrical impedance in the lung region and is a vital indicator for HF progression, as it decreases in the presence of pulmonary fluid. SPO₂ is the measure of blood oxygen saturation and is measured as the percentage of oxygen in the blood. It is an important parameter for evaluating heart function and, hence, a vital indicator for the management of HF. It can also have HF diagnosis and prognostic abilities. According to one study conducted on 220 patients with myocardial infarction, an acute setting in HF, it was found that SPO₂ may have diagnostic and prognostic implications especially when the baseline SPO₂ is less than 93% [26]. A healthy subject has an SPO₂ greater than 95% [27]. Similarly, HR is the measure of the number of heartbeats each minute. In HF, to make up for the lack of blood supply, the heart may beat faster than normal and, therefore, HF patients may have a higher HR than the normal range of 60–100. Moreover, during the progression of HF, patients experience fatigue or swelling in the legs due to a lack of blood supply, which leads to a loss of activity [28]. Therefore, monitoring activity status can help in monitoring and managing HF.

Traditional ICDs measure multiple parameters for the management of HF. The proposed device measures these parameters noninvasively and continuously in real time and is connected with a cloud database. We also developed a Wi-Fi-enabled mobile application (App) in which the data for each patient are stored in the database and can be visualized on the App. We tested this device with 10 subjects in three different real-time conditions such as sitting, standing, and walking. The developed wearable device can

help monitor multiple HF-related parameters in real-time, thus providing more effective disease management.

2. Methods

The device measures parameters related to heart failure including thoracic impedance, HR, SPO₂, and activity status using three different sensors: thoracic impedance sensor, MAX30101, and ADXL 362 [29,30]. The thoracic impedance sensor was built, whereas MAX30101 and ADXL362 are low-cost, off-the-shelf components. This section discusses the development of the body-mounted wearable sensor including the development of the thoracic impedance sensor. It also discusses the protocol of experimentation performed using this device.

Sensor Development

The body-mounted wearable device, as shown in the Figure 1a,b, is housed inside a $70 \times 48 \text{ mm}^2$ 3D casing that can be attached on the chest using a medical-grade double-sided adhesive (DSA). The attachment of the device is shown in Figure 1c. The sensor consists of three different sensors connected to an Arduino MKR 1010 microcontroller. The thoracic impedance sensor and MAX30101 connects with the microcontroller using the I²C protocol, whereas the ADXL 362 connects using the SPI protocol [31,32]. Figure 1d shows a schematic of the thoracic impedance sensor that we developed. The thoracic impedance component is a transthoracic impedance sensor that measures the impedance of the thorax region using a 2-electrode system. These 2 electrodes can be placed across the chest, as shown in the Figure 1c. The thoracic impedance sensor was developed using an AD5933 integrated circuit (IC) from analog devices [33].

The AD5933 is a 12-bit impedance analyzer that sends an AC voltage at a programmable frequency [33]. This voltage can be used to measure unknown impedances. In the case of a two-electrode thoracic impedance system, one electrode is used as an input electrode to send the AC voltage, and the other electrode is used as the output electrode to measure the output voltage. The change in the voltage can be measured to show the impedance of the path between the input and output electrodes. The signal from the AD5933 is very weak and, therefore, requires signal amplification and filtration using the analog front end (AFE), as show in Figure 1d. The AFE is based on an active high-pass filter to filter any DC components, followed by an operational amplifier to form voltage-controlled current source (VCCS) and instrumentation amplifier. The VCCS injects a constant current into the thoracic region to create a potential difference in that region. This potential difference is measured using an instrumentation amplifier and then sent back to the AD5933 to calculate the thoracic impedance based on the generated current and the potential created by the current. Figure 1e shows the circuit of the thoracic impedance sensor consisting of the AD5933 and the AFE.

The MAX30101 measures the HR and SPO₂ using a photoplethysmography (PPG) technique in which an LED with an infrared ray (IR) shines over the arterial periphery to measure the absorption of the input ray [29]. The amount of absorbed light provides the HR and SPO₂. The ADXL 362 is a tri-axial accelerometer for measuring static and dynamic accelerations and is used to detect the activity whenever there is significant motion by the subject [30]. The ADXL 362 can be programmed with activity and inactivity thresholds in terms of codes for the purpose of defining the activity. Whenever the acceleration of the subject is higher than the activity threshold, the accelerometer will register it as an activity. For this purpose, we defined our activity threshold with 300 codes at a default output data rate (ODR) of 100 Hz. This activity threshold was found to be sensitive enough to detect the transition of the subject from a resting to active condition. In the wearable sensor we used binary states for activity, where 1 indicates an active state and 0 indicates an inactive state. These sensors are integrated with the Arduino MKR 1010, and the data are sent to Google Firebase. In this cloud-based database, a Wi-Fi-based mobile application, developed using JavaScript, reads data for the patients and the medical practitioner, which can be

viewed in separate portals [34,35]. The code for the device and data transmission to Google Firebase can be found written in the Arduino IDE (see Supplementary Material Section S1). The program for the wearable is an effective program that consumes only 62,100 bytes, constituting only 23% of the total flash memory of the microcontroller with 32 kilobytes (KB) of static RAM (SRAM) [34]. The device is powered using a small 3.7 V battery with a 1300 mAh capacity. The device consumes 72.35 mA and, therefore, can run on the battery for approximately 18 h. The device was evaluated on subjects of varying biometric and anatomical structures, the results of which are discussed in the subsequent sections.

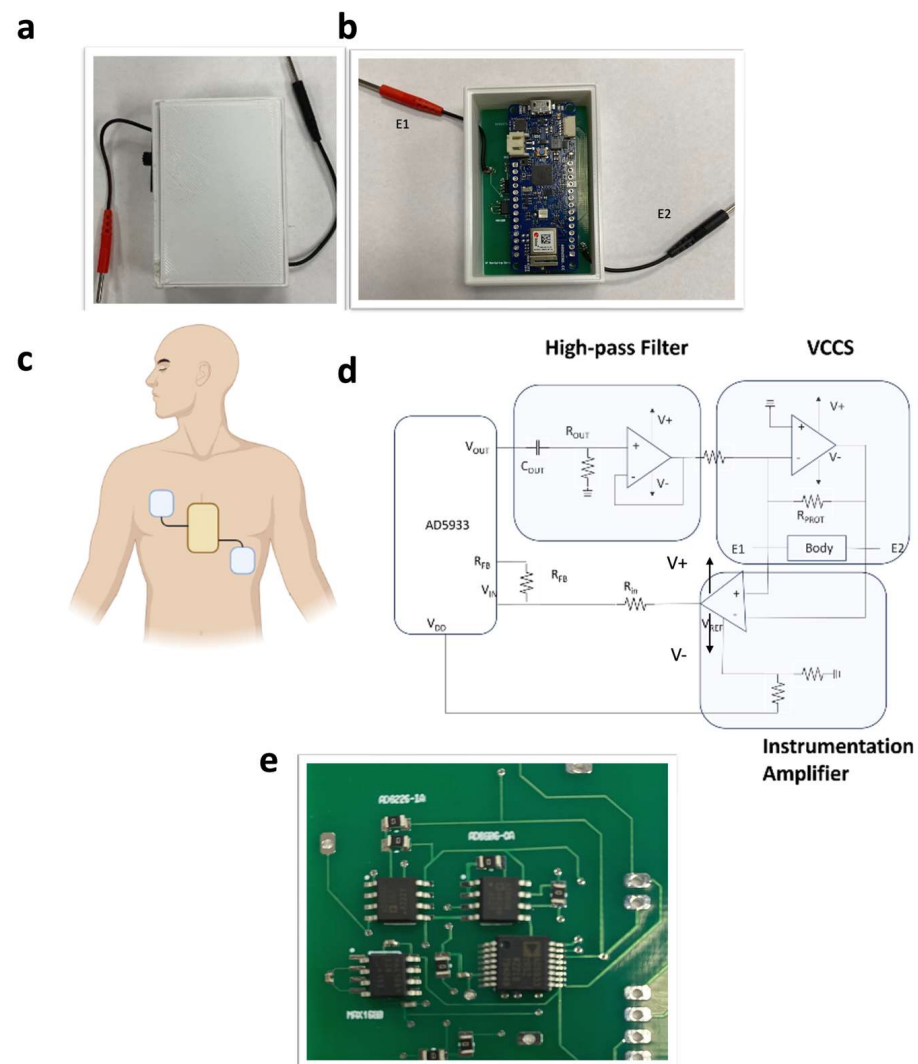


Figure 1. (a) Body-mounted sensor; (b) body-mounted sensor with transthoracic impedance electrodes (E1 and E2); (c) placement of the wearable device and electrodes on the thorax region; (d) schematic of the transthoracic impedance sensor; (e) printed circuit board for the transthoracic impedance sensor.

3. Skin Patch

Along with the body-mounted sensor, we also developed a skin patch by transforming the body-mounted sensor using a flexible PCB, as shown in Figure 2. The skin patch sensor is also an IoT device with the same circuitry but on a flexible PCB which makes it much lighter and more flexible than the body-mounted sensor. Additionally, the skin patch sensor does not have electrode leads wires like the body-mounted sensor and instead connects electrode pads for the thoracic impedance sensor using snap connectors. This provides

much more compliance when using the sensor and removes any noncompliance due to the electrode lead wires.

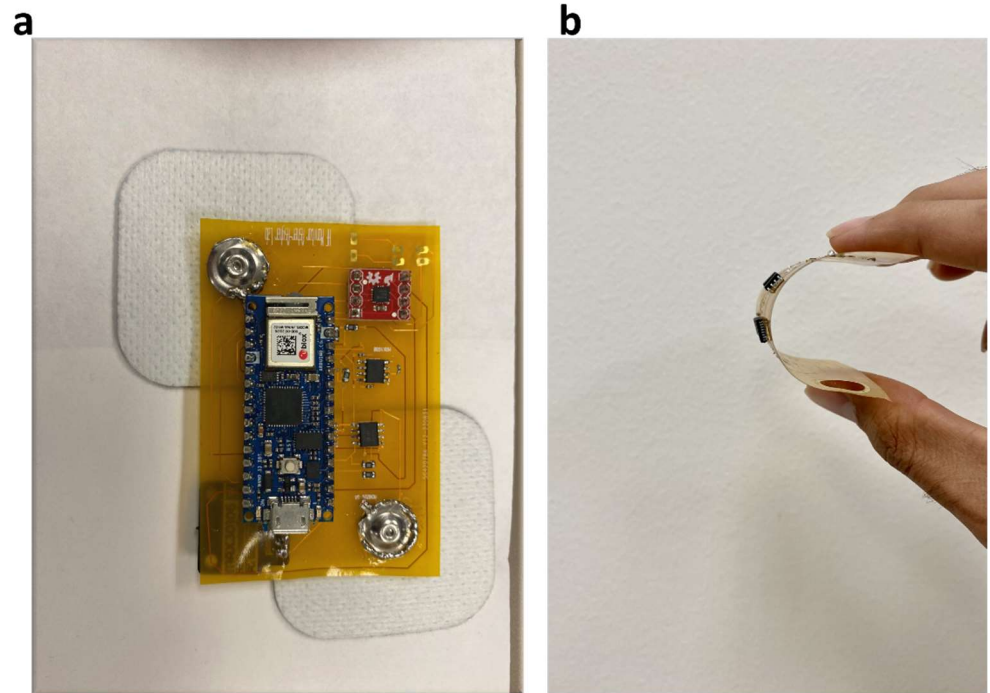


Figure 2. (a) Skin patch sensor; (b) skin patch sensor on flexible PCB.

4. Experimentation

This section will discuss the calibration of the transthoracic impedance sensor, as well as the results of the evaluation of the device on different subjects. The protocol of the experiment is explained in Table 1. The aforementioned vitals of 10 different subjects (6 females and 4 males) were recorded using the device in three different conditions—sitting, standing, and walking—each for 20 min. This was done to evaluate the performance of the device in real-time conditions and for longer periods. All experiments were conducted with the approval of the Institutional Review Board (IRB) from Florida Atlantic University (FAU). For each subject, an account was created in the mobile application with their biometric information, including age, height, and weight. This information is summarized in Table 2. After registration, subjects were asked to sit for 20 min, during which their vitals were recorded and viewed in the mobile application. Similarly, subjects were asked to stand and walk for the next 20 min each.

Table 1. Experimental protocol for recording vitals.

Parameters	Conditions	Duration (min)
Thoracic Impedance Activity Status HR SPO2	Sitting	20
Thoracic Impedance Activity Status HR SPO2	Standing	20
Thoracic Impedance Activity Status HR SPO2	Walking	20

Table 2. Biometric information of subjects.

Subject	Gender	Age	Height (cm)	Weight (lb)
1	M	29	165.1	137
2	M	28	168	120
3	M	31	168	130
4	M	32	167.64	176
5	F	29	161.5	92.59
6	F	31	164	110.231
7	F	30	156	117
8	F	31	171	171.9
9	F	29	158	112
10	F	24	160	105

4.1. Thoracic Impedance Sensor Calibration

The thoracic impedance sensor measures the unknown impedance with reference to the calibration using a known impedance [33,36]. The calibration provides a gain factor that is used to measure the unknown impedance. The known impedance is chosen based on its relevance with the unknown impedance. For this purpose, we chose an RC circuit, as shown in Figure 3a, as it resembles the thorax region [37]. As the thoracic region responds to frequencies between 1 and 100 K, therefore, we programmed the thoracic impedance sensor at 50 KHz (a commonly used frequency for monofrequency thoracic impedance systems) with V_{out} set to be $2V_{pk-pk}$. The values from the sensor were co-related with the standard LCR meter (E4980AL Precision LCR Meter by Keysight Technologies, US) [38]. An equation based on this relationship, as shown in Figure 3b, is used as a gain factor for the unknown impedances. We evaluated the performance of the thoracic impedance sensor by performing respiratory experiments. During inhalation, the air fills the thorax region, and because air is more resistive, it increases the amplitude of the thoracic impedance. This can be seen in Figure 3c. This signal is further processed with normalization and smoothing techniques to obtain a clean signal, as shown in Figure 3d. Moreover, the high-frequency components are removed using empirical mode decomposition [39]. The final signal with respiration peaks is shown in Figure 3e. The frequency spectrum of the cleaned signal is shown in Figure 3f, which shows frequencies of less than 0.5 Hz. It can be seen in the inset plot that the major peak was at 0.16 Hz, which is the frequency of the respiration signal [40].

4.2. Results

The required parameters were recorded for one hour using the protocol mentioned in Table 1. The biometric information of the subjects is shown in Table 2. All subjects were in the age range of 24–31 years. As the experiments were performed on healthy subjects, therefore, we averaged the healthy ranges of these parameters and ignored outliers to avoid any noise in the parameters. For this purpose, the impedance values outside the thoracic impedance range of 70–1120 were filtered to avoid outliers due to skin resistance or loose contact of the electrode pads. Similarly, HR and SPO2 were preprocessed within 60–120 and >95%, respectively. The values outside this range are because of the uneven contact of the optical sensor with the skin.

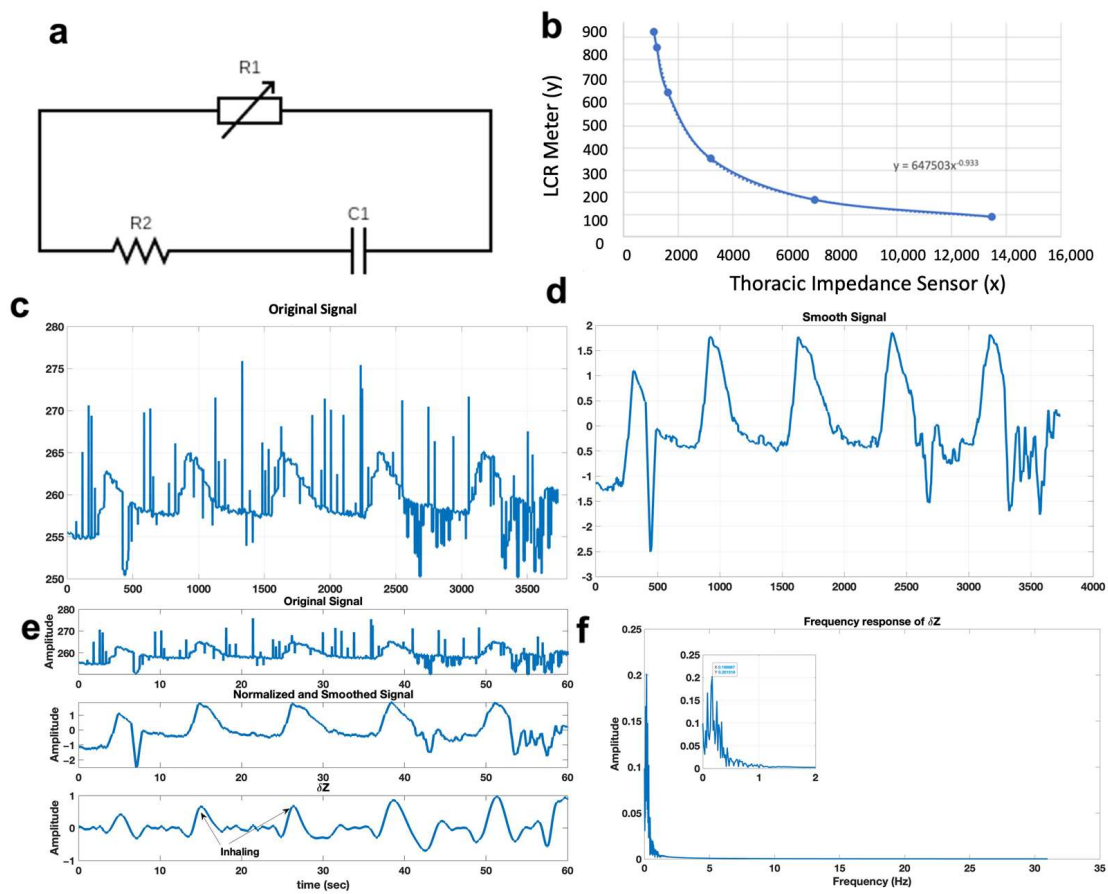


Figure 3. (a) Circuit diagram for the calibration of the transthoracic impedance sensor; (b) fit line equation for calibrating the transthoracic impedance sensor; (c) raw signal of the transthoracic impedance during inspiration; (d) normalized and smoothed signal; (e) clean signal along with the original and smoothed signal highlighting a change in the transthoracic impedance during inspiration; (f) frequency response of the transthoracic impedance signal.

Figure 4 shows the vitals of a subject in different real-time conditions of sitting, standing, and walking. The change in binary state for activity status in Figure 4b, from resting (sitting and standing) to walking, represents the change in the status of activity of the subject. The average values of all subjects’ vitals under the three different conditions are also shown in Table 3, whereas the raw data for all subjects are given in the Supplementary Information Section S2. Figure 5 shows the average values of the vitals for different subjects under the three different conditions. It can be seen in Figure 5b that, on average, males had a higher thoracic impedance than females, where blue, orange and grey boxplots represent three different conditions sitting, standing and walking. This is because of the difference in the body-to-weight index, defined as shown in Equation (1) [41]. The male volunteers had higher BMIs compared to the female volunteers, as is also evident from their biometric information in Table 2. An increased BMI increases the resistivity of the subject and, hence, the thoracic impedance of the thoracic region, according to Equation (2) [42,43]. Similarly, Figure 5c,d show the average SPO2 and HR for the subjects. As expected, on average, the HRs in the resting conditions (i.e., sitting and standing) were lower than the condition in which the subject was walking, as shown in Figure 5e.

$$BMI = \frac{Weight}{Height^2} \tag{1}$$

$$R = \frac{\rho L}{A} \tag{2}$$

where p is the resistivity region, L is the length, and A is the cross-sectional area of the region.

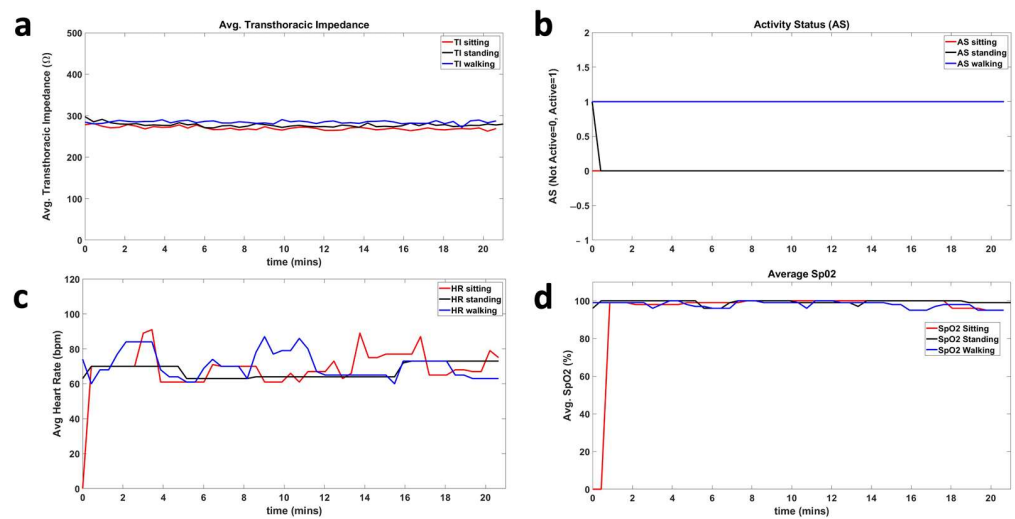


Figure 4. (a) Average transthoracic impedance of a subject in the different conditions; (b) activity status of a subject in the different conditions; (c) average heart rate of a subject in the different conditions; (d) average SPO2 of a subject in the different conditions.

Table 3. Average values of the vitals for subjects in different conditions.

	Avg TI			SPO2			Avg HR			Activity Status		
	Sitting	Standing	Walking	Sitting	Standing	Walking	Sitting	Standing	Walking	Sitting	Standing	Walking
	269.9	277.6	284.5	98.9	99.3	99	69.9	67.3	70.4	0	0	1
	218.3	231.3	236.6	98.3	97.9	99.1	68.8	79.7	105.0	0	0	1
	223.1	216.0	220.7	99.6	98.4	98.7	70.0	64.9	89.2	0	0	1
	287.1	295.6	291.3	98.8	99.5	97.5	66.5	74.9	71.3	0	0	1
	190.1	195.9	196.3	97.7	97.1	98.5	76.9	81.5	86.5	0	0	1
	221.2	229.6	231.6	98.7	98.4	97.8	61.9	67.2	75.4	0	0	1
	210.1	217.4	218.1	97.1	97.3	98.5	67.1	65.4	74.5	0	0	1
	268.8	280.2	291.1	99.1	99.7	98.3	65.9	64.7	82.8	0	0	1
	242.6	245.2	239.9	98.6	98.9	97.7	66.9	62.7	78.9	0	0	1
	226.4	228.9	230.8	99.5	97.1	98.6	77.3	75.7	73.0	0	0	1

The same experimentation was performed with a healthy subject (S1), the results of which are shown in Figure 6, using the skin patch to measure vital parameters. Figure 6 shows the parameter results of the subject using the skin patch. It can be seen that similar results were obtained for the subject, using the skin patch, from the body-mounted sensor, except that the magnitude of the thoracic impedance of the subject was lower than the magnitude of the thoracic impedance of the subject using the body-mounted sensor. This is because of the decrease in the distance between the electrode pads in the skin patch due to the snap connectors, which essentially represent the length of the area for which the impedance is measured. As the length of the region under consideration has decreased therefore according to Equation (2) its magnitude will also decrease, keeping other factors constant. Moreover, similar results for the rest of the parameters were obtained in which the activity status transitions accordingly from not active to an active state in resting to walking conditions, and the HR along with SPO2 were in the expected ranges of 60–100 bpm and >95%, respectively, as well.

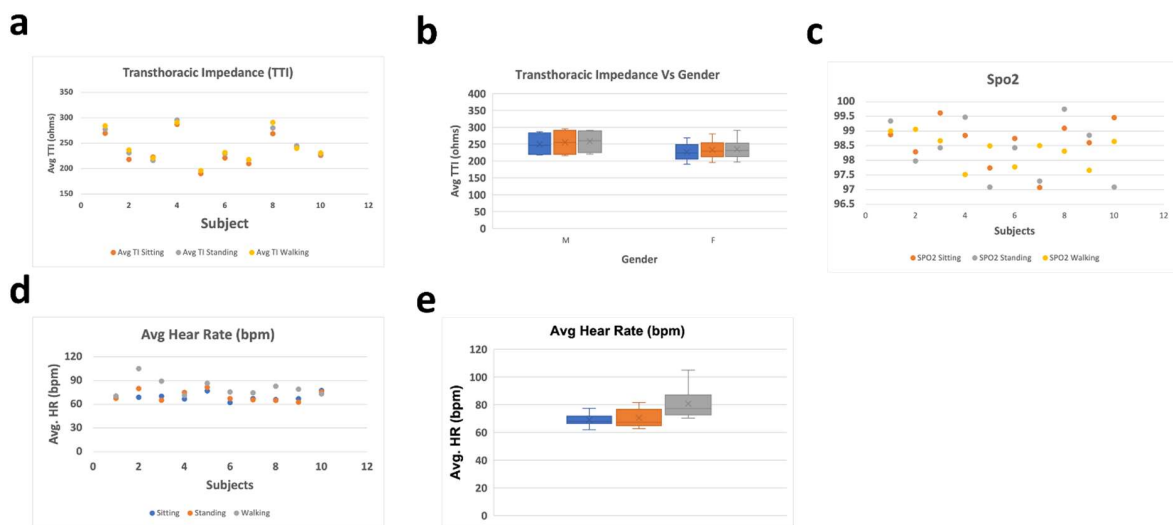


Figure 5. (a) Average transthoracic impedance while sitting, standing, and walking; (b) average transthoracic impedance vs. gender; (c) average SPO2 while sitting, standing, and walking; (d) average heart rate for subjects while sitting, standing, and walking; (e) average heart rate in three different conditions.

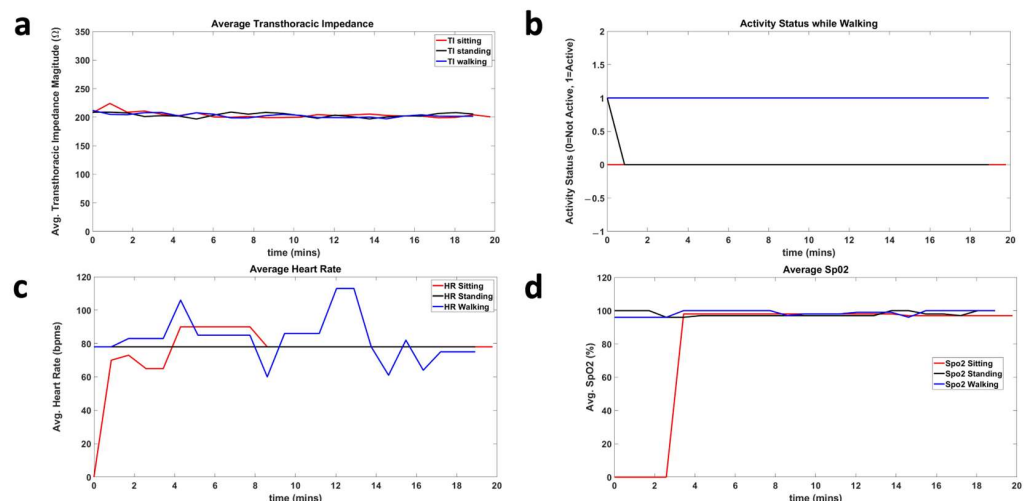


Figure 6. (a) Average transthoracic impedance of a subject while sitting; (b) activity status of a subject while sitting; (c) average heart rate of a subject while sitting; (d) average SPO2 of a subject while sitting.

5. Discussion

A novel body-mounted wearable sensor has been developed to monitor vital parameters related to HF management. The device is an IoT device that monitors parameters related to HF and communicates them over Wi-Fi, whereby the parameters can be visualized in a mobile application. The device was evaluated in real-life conditions, where it was found to successfully measure these vitals in real time and continuously. The device consists of different sensors, including a thoracic impedance sensor, an optical sensor for HR and SPO2, and an accelerometer for activity status. The thoracic impedance sensor was built using the AD5933 impedance analyzer, and thoracic impedance was measured using an AFE. The thoracic impedance sensor’s performance was validated using a standard respiration test, whereby the thoracic impedance increased in the presence of inspiration. Furthermore, the device was then evaluated on 10 different subjects, whereby their vitals were recorded for 1 h under different real-life conditions, namely, sitting, standing, and walking.

It was observed that, on average, males have higher thoracic impedance than females, and the resting HRs of the subjects were lower than their HR during walking. Similarly, the device successfully kept track of the activity status of the subjects. The device is a small $70 \times 45 \text{ mm}^2$ compact sensor that can be mounted on the chest with two electrodes across the thorax. The device has the potential to be made into an electronic skin (e-skin), and we showed one possibility of this by making it over a flexible PCB. This will further reduce the size and height of the device.

The device can be used as a telehealth monitor when connected with a cloud database and a Wi-Fi-based mobile application. The mobile application has different portals for medical practitioners and patients, protected with their username and password, as shown in Figure 7 [44]. With the increasing economic burden of cardiovascular diseases, especially HF, telehealth monitoring may help to reduce hospital visits and increase the accessibility of patients' vital parameters. This noninvasive sensor is a novel device that can help patients and providers manage HF with real-time monitoring. Multiparametric analysis allows for better specificity and sensitivity toward disease diagnostics [45]. Thoracic impedance alone has been found to have a sensitivity of 62% and a prognostic ability to detect heart failure, on average, 18 days before it occurs [45,46]. This proposed multiparametric device measures thoracic impedance along with other vital parameters that can improve management of HF using a telemedicine system. Recent efforts have been made to monitor HF using wearable devices. For example, a wearable vest has been developed to monitor transthoracic impedance along with ECG [23,47]. However, unlike the device proposed in this paper, it can only be used with the patient at rest. Similarly, a body-mounted sensor has also been developed to monitor HF using time synchronized vibrations, but it is not recommended to use while performing daily tasks [24,48]. Therefore, the device proposed in this article has the ability to measure parameters important in monitoring HF, continuously and in real-time conditions to better understand HF progression.

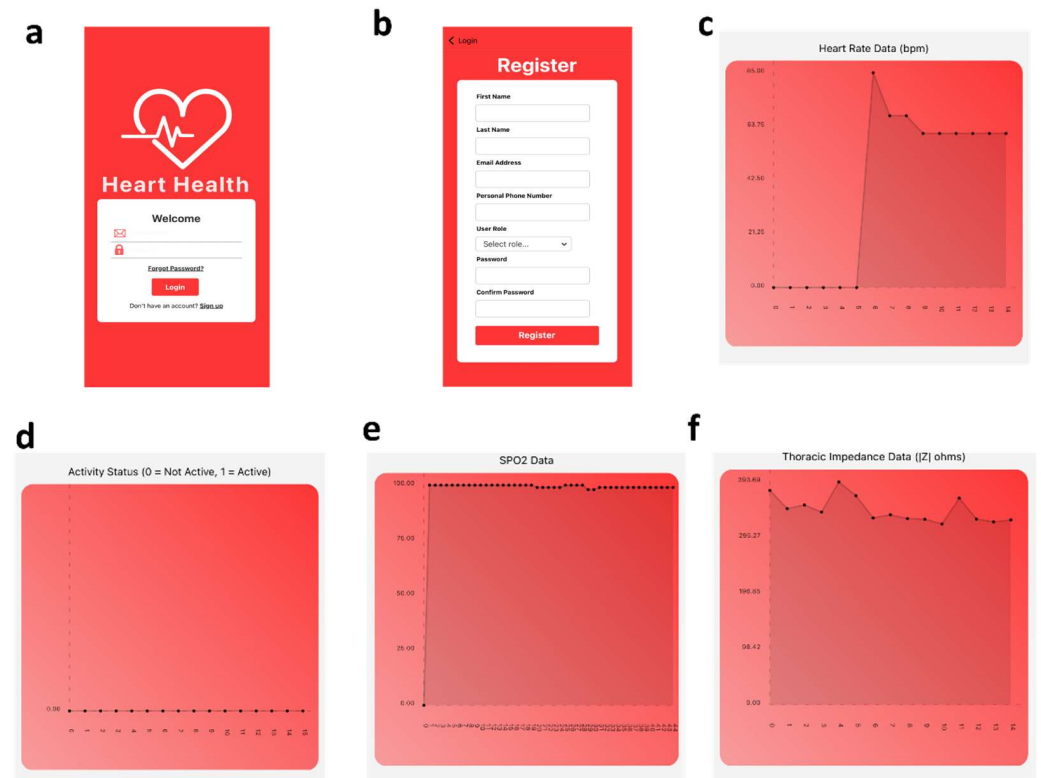


Figure 7. (a) Mobile application sign-in page; (b) mobile application registration page; (c) heart rate of a subject; (d) activity status of a subject; (e) SPO2 of a subject; (f) transthoracic impedance of a subject while walking.

6. Conclusions

In this paper, we discussed the development and evaluation of a noninvasive IoT wearable device that measures vitals related to HF, namely, thoracic impedance, HR, SPO₂, and activity status. The device conveniently attaches to the chest using a medical-grade double-sided adhesive (DSA) and measures vitals continuously in real time. These vitals are stored in a cloud database and visualized using a Wi-Fi-based mobile application. The device was validated by recording vitals for 1 h in 10 different subjects in sitting, standing, and walking conditions. The device was able to successfully record and process the monitored data in the expected ranges. We also report an extended version of the body-mounted sensor, a flexible skin patch, which is more lightweight and patient compliant than the body-mounted sensor, with a comparable performance as that of the body-mounted sensor.

Supplementary Materials: The following supporting information can be downloaded at: <https://www.mdpi.com/article/10.3390/iot5010008/s1>.

Author Contributions: S.M.A.I., Conceptualization, Study Design, Methodology, Investigation, Formal analysis, and Writing—Original Draft and Editing; I.M., Review and Editing; M.A.L., Review and Editing; W.A., Conceptualization, Study Design, Review and Editing, Supervision, Project Administration, and Funding Acquisition. All authors have read and agreed to the published version of the manuscript.

Funding: This research was funded by the NSF CAREER Award 1942487, NIH R61AI127214, and the seed award from the I-SENSE Institute, and College of Engineering and Computer Science, Florida Atlantic University, Boca Raton, FL.

Informed Consent Statement: Informed consent was obtained from all subjects involved in the study.

Data Availability Statement: The datasets generated during and/or analyzed during the current study are available from the corresponding author upon reasonable request. They are also provided in the Supplementary Information.

Conflicts of Interest: The authors of this study have no conflicts of interest to declare.

References

1. NHS Inform. Cardiovascular Disease—Illnesses & Conditions. Available online: <https://www.nhsinform.scot/illnesses-and-conditions/heart-and-blood-vessels/conditions/cardiovascular-disease> (accessed on 14 July 2023).
2. Heart Failure Facts & Information. Available online: <https://hfsa.org/patient-hub/heart-failure-facts-information> (accessed on 14 July 2023).
3. Yan, T.; Zhu, S.; Yin, X.; Xie, C.; Xue, J.; Zhu, M.; Weng, F.; Zhu, S.; Xiang, B.; Zhou, X.; et al. Burden, Trends, and Inequalities of Heart Failure Globally, 1990 to 2019: A Secondary Analysis Based on the Global Burden of Disease 2019 Study. *J. Am. Heart Assoc.* **2023**, *12*, 27852. [CrossRef] [PubMed]
4. Mayo Clinic. Pulmonary Edema—Symptoms & Causes. Available online: <https://www.mayoclinic.org/diseases-conditions/pulmonary-edema/symptoms-causes/syc-20377009> (accessed on 14 July 2023).
5. American Heart Association. Types of Heart Failure. Available online: <https://www.heart.org/en/health-topics/heart-failure/what-is-heart-failure/types-of-heart-failure> (accessed on 31 October 2023).
6. American Heart Association. Devices That May Interfere with ICDs and Pacemakers. Available online: <https://www.heart.org/en/health-topics/arrhythmia/prevention--treatment-of-arrhythmia/devices-that-may-interfere-with-icds-and-pacemakers> (accessed on 21 May 2023).
7. Medtronic. Cardiac Monitors—Reveal LINQ ICM System. Available online: <https://www.medtronic.com/us-en/healthcare-professionals/products/cardiac-rhythm/cardiac-monitors/reveal-linq-icm.html> (accessed on 20 June 2023).
8. Medtronic. The CareLink Network—Information Systems. Available online: <https://www.medtronic.com/us-en/healthcare-professionals/products/cardiac-rhythm/managing-patients/information-systems/carelink-network.html> (accessed on 14 July 2023).
9. Medtronic. Patient Management—Cardiac Device CareLink Network. Available online: <https://www.medtronic.com/ca-en/healthcare-professionals/products/cardiac-rhythm/patient-management-carelink/medtronic-carelink-network-cardiac-device-patients.html> (accessed on 10 May 2023).
10. Abbott. How the CardioMEMS HF System and Merlin.net PCN Works. Available online: https://www.cardiovascular.abbott/us/en/hcp/products/heart-failure/pulmonary-pressure-monitors/cardiomems/about/how-it-works.html?gclid=CjwKCAjwh8mlBhB_EiwAsztdBCTDS73LGEUvOYK6ae3FRJe_THVaSifd5ab6Zyq8_H1gsz4H2Lu0hoCH9EQAvD_BwE (accessed on 14 July 2023).

11. DAIC. ICD Manufacturers Must Increase Battery Life to Cut Costs, Improve Care. Available online: <https://www.dicardiology.com/article/icd-manufacturers-must-increase-battery-life-cut-costs-improve-care> (accessed on 21 May 2023).
12. Schmier, J.K.; Ong, K.L.; Fonarow, G.C. Cost-Effectiveness of Remote Cardiac Monitoring With the CardioMEMS Heart Failure System. *Clin. Cardiol.* **2017**, *40*, 430. [CrossRef] [PubMed]
13. Iqbal, S.M.A.; Mahgoub, I.; Du, E.; Leavitt, M.A.; Asghar, W. Advances in healthcare wearable devices. *npj Flex. Electron.* **2021**, *5*, 1. [CrossRef]
14. Bonato, P. Advances in wearable technology and its medical applications. In Proceedings of the 2010 Annual International Conference of the IEEE Engineering in Medicine and Biology, Buenos Aires, Argentina, 31 August–4 September 2010.
15. Stehlik, J.; Schmalfluss, C.; Bozkurt, B.; Nativi-Nicolau, J.; Wohlfahrt, P.; Wegerich, S.; Rose, K.; Ray, R.; Schofield, R.; Deswal, A.; et al. Continuous wearable monitoring analytics predict heart failure hospitalization: The link-hf multicenter study. *Circ. Heart Fail.* **2020**, *13*, e006513. [CrossRef] [PubMed]
16. What Is the Internet of Things (IoT)? Available online: <https://www.oracle.com/internet-of-things/what-is-iot/> (accessed on 24 February 2024).
17. IEEE Pulse. IoMT (Internet of Medical Things): Reducing Cost While Improving Patient Care. Available online: <https://www.embs.org/pulse/articles/iomt-internet-of-medical-things-reducing-cost-while-improving-patient-care/> (accessed on 24 February 2024).
18. Haghi Kashani, M.; Madanipour, M.; Nikravan, M.; Asghari, P.; Mahdipour, E. A systematic review of IoT in healthcare: Applications, techniques, and trends. *J. Netw. Comput. Appl.* **2021**, *192*, 103164. [CrossRef]
19. Wang, S.; Bi, S.; Zhang, L.; Liu, R.; Wang, H.; Gu, J. Skin-inspired antibacterial conductive hydrogels customized for wireless flexible sensor and collaborative wound healing. *J. Mater. Chem. A Mater.* **2023**, *11*, 14096–14107. [CrossRef]
20. Xu, J.; Wang, H.; Wen, X.; Wang, S.; Wang, H. Mechanically Strong, Wet Adhesive, and Self-Healing Polyurethane Ionogel Enhanced with a Semi-interpenetrating Network for Underwater Motion Detection. *ACS Appl. Mater. Interfaces* **2022**, *14*, 54203–54214. [CrossRef] [PubMed]
21. Chen, K.; Liang, K.; Liu, H.; Liu, R.; Liu, Y.; Zeng, S.; Tian, Y. Skin-Inspired Ultra-Tough Supramolecular Multifunctional Hydrogel Electronic Skin for Human–Machine Interaction. *Nanomicro Lett.* **2023**, *15*, 102. [CrossRef] [PubMed]
22. Liu, R.; Liu, Y.; Cheng, Y.; Liu, H.; Fu, S.; Jin, K.; Li, D.; Fu, Z.; Han, Y.; Wang, Y.; et al. Aloe Inspired Special Structure Hydrogel Pressure Sensor for Real-Time Human-Computer Interaction and Muscle Rehabilitation System. *Adv. Funct. Mater.* **2023**, *33*, 2308175. [CrossRef]
23. Dovancescu, S.; Saczynski, J.S.; Darling, C.E.; Riistama, J.; Kuniyoshi, F.S.; Meyer, T.; Goldberg, R.; McManus, D.D. Detecting Heart Failure Decompensation by Measuring Transthoracic Bioimpedance in the Outpatient Setting: Rationale and Design of the SENTINEL-HF Study. *JMIR Res. Protoc.* **2015**, *4*, e121. [CrossRef] [PubMed]
24. Hemotag. Rapid Vitals for Monitoring Structural Heart Health. Available online: <https://hemotag.com/> (accessed on 3 February 2024).
25. PubMed. A Usability Study of a Mobile Monitoring System for Congestive Heart Failure Patients. Available online: <https://pubmed.ncbi.nlm.nih.gov/25160241/> (accessed on 3 February 2024).
26. Masip, J.; Gayà, M.; Páez, J.; Betbesé, A.; Vecilla, F.; Manresa, R.; Ruiz, P. Pulse Oximetry in the Diagnosis of Acute Heart Failure. *Rev. Española Cardiol. (Engl. Ed.)* **2012**, *65*, 879–884. [CrossRef] [PubMed]
27. MN Department of Health. Oxygen Levels, Pulse Oximeters, and COVID-19. Available online: <https://www.health.state.mn.us/diseases/coronavirus/pulseoximeter.html> (accessed on 31 October 2023).
28. Penn Medicine. Exercise & Activity for Patients with Heart Failure. Available online: <https://www.pennmedicine.org/updates/blogs/heart-and-vascular-blog/2015/july/5-tips-for-exercise-with-heart-failure> (accessed on 17 July 2023).
29. SparkFun. Photodetector Breakout—MAX30101 (Qwiic)—SEN-16474—SparkFun Electronics. Available online: <https://www.sparkfun.com/products/16474> (accessed on 21 May 2023).
30. Devices, A. Micropower, 3-Axis, ± 2 g/ ± 4 g/ ± 8 g Digital Output MEMS Accelerometer ADXL362. Available online: <https://www.analog.com/media/en/technical-documentation/data-sheets/adxl362.pdf> (accessed on 16 July 2023).
31. Basics of the I2C Communication Protocol. Available online: <https://www.circuitbasics.com/basics-of-the-i2c-communication-protocol> (accessed on 16 July 2023).
32. Basics of the SPI Communication Protocol. Available online: <https://www.circuitbasics.com/basics-of-the-spi-communication-protocol> (accessed on 16 July 2023).
33. Devices A. MSPS, 12-Bit Impedance Converter, Network Analyzer AD5933. Available online: <https://www.analog.com/media/en/technical-documentation/data-sheets/AD5933.pdf> (accessed on 16 July 2023).
34. Arduino Online Shop. Arduino MKR WiFi 1010. Available online: <https://store-usa.arduino.cc/products/arduino-mkr-wifi-1010> (accessed on 11 May 2023).
35. Firebase. Available online: https://firebase.google.com/?gad=1&gclid=CjwKCAjw9pGjBhB-EiwAa5jI3KycMFGWjGE_t6A8_G_ZhAsbRyKNtqcDcqUWhCkMU_PUO_ioOCffAhoCefwQAvD_BwE&gclidsrc=aw.ds (accessed on 16 May 2023).
36. Iqbal, S.M.A.; Mahgoub, I.; Du, E.; Leavitt, M.A.; Asghar, W. Development of a wearable belt with integrated sensors for measuring multiple physiological parameters related to heart failure. *Sci. Rep.* **2022**, *12*, 20264. [CrossRef] [PubMed]
37. Aqueveque, P.; Gómez, B.; Monsalve, E.; Germany, E.; Ortega-Bastidas, P.; Dubo, S.; Pino, E.J. Simple Wireless Impedance Pneumography System for Unobtrusive Sensing of Respiration. *Sensors* **2020**, *20*, 5228. [CrossRef] [PubMed]

38. TestEquity. Keysight E4980AL/032 Precision LCR Meter—300 kHz. Available online: https://www.testequity.com/product/22137-1-E4980AL-032?gclid=Cj0KCQjwzdOIBhCNARIsAPMwjby6wZYxrFeHvnX4rxsLX3PTZpulMSzP5S6WtuB07ixiKrFLxPqdtgYaAtr2EALw_wcB (accessed on 16 July 2023).
39. MATLAB. Empirical Mode Decomposition. Available online: <https://www.mathworks.com/discovery/empirical-mode-decomposition.html> (accessed on 31 October 2023).
40. Jarchi, D.; Salvi, D.; Tarassenko, L.; Clifton, D.A. Validation of Instantaneous Respiratory Rate Using Reflectance PPG from Different Body Positions. *Sensors* **2018**, *18*, 3705. [[CrossRef](#)] [[PubMed](#)]
41. Physics LibreTexts. 9.4: Resistivity and Resistance. Available online: [https://phys.libretexts.org/Bookshelves/University_Physics/Book:_University_Physics_\(OpenStax\)/Book:_University_Physics_II_-_Thermodynamics_Electricity_and_Magnetism_\(OpenStax\)/09:_Current_and_Resistance/9.04:_Resistivity_and_Resistance](https://phys.libretexts.org/Bookshelves/University_Physics/Book:_University_Physics_(OpenStax)/Book:_University_Physics_II_-_Thermodynamics_Electricity_and_Magnetism_(OpenStax)/09:_Current_and_Resistance/9.04:_Resistivity_and_Resistance) (accessed on 31 October 2023).
42. PubMed. Transthoracic Impedance: Differences between Men and Women with Implications for Impedance Cardiography. Available online: <https://pubmed.ncbi.nlm.nih.gov/7159339/> (accessed on 13 May 2023).
43. CDC-DNPAO. Calculating BMI using the English System—BMI for Age Training Course. Available online: https://www.cdc.gov/nccdphp/dnpao/growthcharts/training/bmiage/page5_2.html (accessed on 31 October 2023).
44. Iqbal, S.M.A.; Leavitt, M.A.; Pedilus, G.; Mahgoub, I.; Asghar. A wearable telehealth system for the monitoring of parameters related to heart failure. *Heliyon*. **2024**, *4*, e26841. [[CrossRef](#)] [[PubMed](#)]
45. Vollmann, D.; Nägele, H.; Schauerte, P.; Wiegand, U.; Butter, C.; Zanotto, G.; Quesada, A.; Guthmann, A.; Hill, M.R.S.; Lamp, B. Clinical utility of intrathoracic impedance monitoring to alert patients with an implanted device of deteriorating chronic heart failure. *Eur. Heart J.* **2007**, *28*, 1835–1840. [[CrossRef](#)] [[PubMed](#)]
46. Yu, C.M.; Wang, L.; Chau, E.; Chan, R.H.W.; Kong, S.L.; Tang, M.O.; Christensen, J.; Stadler, R.W.; Lau, C.P. Intrathoracic impedance monitoring in patients with heart failure: Correlation with fluid status and feasibility of early warning preceding hospitalization. *Circulation* **2005**, *112*, 841–848. [[CrossRef](#)] [[PubMed](#)]
47. Gyllensten, I.C.; Bonomi, A.G.; Goode, K.M.; Reiter, H.; Habetha, J.; Amft, O.; Cleland, J.G.F. Early Indication of Decompensated Heart Failure in Patients on Home-Telemonitoring: A Comparison of Prediction Algorithms Based on Daily Weight and Noninvasive Transthoracic Bio-impedance. *JMIR Med. Inform.* **2016**, *4*, e3. [[CrossRef](#)] [[PubMed](#)]
48. Pino, J.E.; Ramos-Tuarez, F.; Nieves, J.; Sabates, A.; Sehatbakhsh, S.; Pradeep, D.; Torres, P.; Chomko, T.A.; Abdallah, A.; Al Abbasi, B.; et al. Safety And Efficacy of The HemotagTm Recording Device To Detect Acutely Decompensated Heart Failure. *J. Card. Fail.* **2020**, *26*, S45. [[CrossRef](#)]

Disclaimer/Publisher’s Note: The statements, opinions and data contained in all publications are solely those of the individual author(s) and contributor(s) and not of MDPI and/or the editor(s). MDPI and/or the editor(s) disclaim responsibility for any injury to people or property resulting from any ideas, methods, instructions or products referred to in the content.